

## Second-order updating in shape optimization for salt segmentation

Taylor Dahlke, Biondo Biondi, and Robert Clapp

### SUMMARY

Interpretation of sharp salt boundaries can be achieved by using level sets to define the boundary as an isocontour of a higher dimensional implicit surface. Using shape optimization, we can evolve this surface and the boundary it represents. We derive an update for the implicit surface that uses second-order information in the Hessian of the FWI objective function, taking into account the effects of the acquisition, as well as scattering and transmission energy. This approach helps us avoid local minima and more effectively converges on the true model, both in terms of the data and model residual norms. We demonstrate this idea using a Gauss-Newton approximation of the Hessian on synthetic examples.

### INTRODUCTION

Because salt has a higher velocity compared to the surrounding sediments, it is quite reflective. Salt often has complex shapes and high reflectivity, so the energy that strikes it is scattered before it reaches the targets of interest nearby (Etgen et al., 2009). Additionally, this energy may not be properly captured by the acquisition geometry, even with long offsets. If the boundaries of the salt are placed improperly, it becomes especially hard to identify targets along the flanks and base of salt. Furthermore, if a well is inadvertently placed through salt, this could complicate drilling, or the well could fail. For these reasons, it is important to correctly identify the boundaries of salt bodies in our earth models.

Tomographic approaches for interpreting salt bodies can be less than effective, because the results tend to be too smooth to provide significantly accurate placement of the salt boundaries. Manual and semi-automatic picking of salt boundaries are common approaches for interpreting the desired sharp delineations, but these methods can be time-consuming and tedious since expert input is necessary for either the actual picking, or the oversight and correction. Models are usually refined iteratively, which means manual adjustment of the salt bodies must be continuously revisited, causing a bottleneck in the overall work flow. A robust method for further automating the salt interpretation procedure during inversion would prove to be very useful in practice.

Some previous approaches to segmenting salt bodies use a shape optimization approach for evolving the boundaries (Guo and de Hoop, 2013; Lewis et al., 2012). These boundaries can be represented as the zero-isocontour of a higher dimensional surface (for example, a 2D boundary as a contour of a 3D surface). An updating step can be derived to evolve this shape / isosurface according to the Full Waveform Inversion (FWI) objective function. Unlike the smooth boundaries produced by tomographic approaches, the isocontour resulting from shape optimization provides a sharp boundary, which is a more ap-

propriate way to classify many salt-sediment interfaces. Guo and de Hoop (2013) utilize this approach using a frequency domain forward wave operator to evolve a salt boundary and velocity model. Their approach creates and applies a steepest-descent update, which can create problems updating the base-of-salt (BOS) once the top-of-salt (TOS) has gotten close to convergence. This issue has been observed in recent work (Guo and de Hoop, 2013), and is an inherent problem with the steepest-descent update approach. In (Dahlke, 2015), we decomposed the domain of the model so that a line search was performed for both TOS and BOS gradient, allowing the BOS to continue updating after the TOS converged. However, splitting the domain into more regions in order to get better resolution of updating conflicts with the added cost from the line search that each new domain requires. Further, this approach can never take into account the relationships between model points; its application is ultimately a diagonal matrix constrained to  $n$  unique values (in the case of  $n$  domain regions).

To address the problem with steepest-descent updating, we utilize the second-order information provided by the Hessian of the objective function, in order to choose better search directions in our inversion and avoid local minima. We use a Gauss-Newton approximation to the Hessian in our inversion. Further, we suggest the potential of using the scattering and transmission components of the Hessian in order to further improve our updating.

In this paper we will begin by discussing the fundamentals of the level set method, followed by the derivation of the second-order boundary update. Next we will describe and demonstrate the algorithm used, and discuss the assumptions and fundamental limitations of this approach. Last, we will compare the first order updating provided by a steepest-descent approach to second order updating, and demonstrate the improved results that this approach offers.

### THEORY

While it may seem counter-intuitive to add an extra dimension to our problem, by doing so, we gain the advantage of easily merging/separating bodies as the evolution proceeds, as well as the ability to handle sharp corners and cusps in the lower-dimensional (2D) plane on which the boundary exists.

Osher and Sethian (1988) and Burger (2003) describe the level set of an implicit surface  $\phi$  that represents the salt body boundary as  $\phi(x_{\Gamma}, \tau) = 0$ , where  $x_{\Gamma}$  is the set of points along a boundary  $\Gamma$ , and  $\tau$  is the iteration count. By taking the derivative of this equation with respect to  $\tau$  (to find the  $\delta\phi$  between iterations), applying the chain rule, and re-arranging terms we can get:

## Second-order shape optimization

$$\frac{\partial \phi}{\partial \tau} = -V(x_\Gamma, \tau) |\nabla \phi|. \quad (1)$$

The scalar speed term  $V(x_\Gamma, \tau)$  describes the magnitude of the variation of  $\phi$  that is normal to the boundary  $\Gamma$ . It determines the evolution of the implicit surface, and ultimately the boundary implied by it. We derive this normal velocity such that the FWI objective function is minimized

$$\psi = \min \|F(m) - d\|_2^2, \quad (2)$$

where  $F(\cdot)$  is the forward wavefield modeling operator,  $m$  is the velocity model, and  $d$  is the observed data.

### Calculus of variations

The shape derivative we use is based on a formal calculus of variations outlined in Santosa (1996). The objective is to define the variation of the model  $m$  with respect to the boundary variation (represented implicitly by the surface,  $\phi$ ).

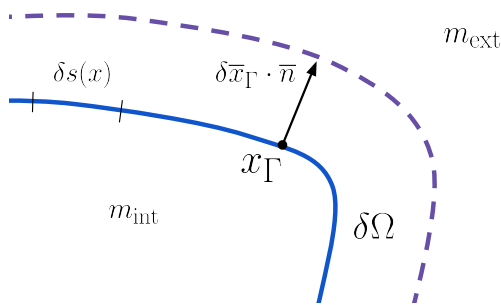


Figure 1: The geometry of the curve  $\{x_\Gamma : \phi = 0\}$  for a variation  $\delta\phi(x)$  for an evolution step  $\tau$ .  $\delta\Omega$  is the perturbation of the salt body  $\Omega$ .

Figure 1 illustrates that  $\delta m(x_\tau)$  will be  $\pm(m_{\text{int}} - m_{\text{ext}})$ , depending on the relative values of  $m_{\text{int}}$  and  $m_{\text{ext}}$  or the sign (direction) of the normal vector  $\vec{n}$ . We only care about the component of  $\delta x_\Gamma$  that occurs in the normal direction, because a tangential variation of  $x_\Gamma$  does not affect  $m$  or  $\phi$ . Because of this, we can express  $\delta m(x)$  as

$$\delta m(x) = (m_{\text{int}} - m_{\text{ext}}) \delta \vec{x}_\Gamma \cdot \vec{n} \Big|_{x \in \partial\Omega}. \quad (3)$$

which can be considered a measure over  $\partial\Omega$ .

We consider an inner product of velocity model perturbation  $\delta m$  with a test function  $f(x)$ . Formally, this can be written as,

$$\langle \delta m, f(x) \rangle = \int_{\mathbb{R}^2} \delta m(x) f(x) dx = \int_{\partial\Omega} \delta m(x) f(x) dx. \quad (4)$$

Because the  $\delta m(x)$  term equals zero in  $\mathbb{R}^2 \setminus \partial\Omega$ , it does not contribute to the overall inner product when integrating over

that domain; therefore, we only integrate over  $\partial\Omega$  where  $\delta m(x)$  is non-zero.

We want to decrease our objective function (2), so we choose a second-order Newton step such that  $\Delta m = -H^{-1}g$ . In the case of the FWI objective function, we can use the Gauss-Newton approximation of the Hessian such that

$$\Delta m = -[B^T(m_0)B(m_0)]^{-1}g, \quad (5)$$

where  $B(m_0)$  is the linearized Born operator at  $m = m_0$ , and  $g = B^T(m_0)r$  is the adjoint Born operator applied to the data space residuals, as described in Plessix (2006). Since this is the best search direction to decrease our objective function (2) in the quadratic sense, we substitute it into  $f(x)$  from (4) to get

$$\langle \delta m, f(x) \rangle = \int_{\partial\Omega} \delta m \left( [B^T(m_0)B(m_0)]^{-1} B(m_0)r \right) dx. \quad (6)$$

Because we are interested in the projection of this search direction on the constraining equation for  $\delta m$  that we outline in equation (3), we make our substitution for  $\delta m$  yielding to:

$$\langle \delta m, f(x) \rangle = \int_{\partial\Omega} (m_{\text{int}} - m_{\text{ext}}) \delta \vec{x}_\Gamma \cdot \vec{n} \left( [B^T(m_0)B(m_0)]^{-1} B(m_0)r \right) ds(x). \quad (7)$$

Because  $\delta x_\Gamma$  is infinitesimal, we replace  $dx$  with  $\delta \vec{x}_\Gamma \cdot \vec{n}$  when we substitute into (7). We call  $ds(x)$  the incremental arc length along the boundary  $\Gamma$ . We can think of  $\delta \vec{x}_\Gamma \cdot \vec{n} ds(x)$  as roughly the incremental area over which  $m$  varies at  $x$ .

We remember that in the previous section we stated the goal of this derivation as being a solution of the scalar velocity function  $V(x_\Gamma, \tau)$ , such that the objective function is minimized. We recognize that the normal component of the variation  $\delta x_\Gamma$  satisfies:

$$\delta \vec{x}_\Gamma \cdot \vec{n} = V(x_\Gamma, \tau). \quad (8)$$

In order for the inner product that we have defined in (7) to represent a decrease in the objective function (2), we need to choose a  $V(x_\Gamma, \tau)$  such that  $\langle \delta m, f(x) \rangle < 0$ . The choice of  $V(x_\Gamma, \tau)$  that give us the most negative value is opposite to the other terms, i.e;

$$V(x_\Gamma, \tau) = - \int_{\partial\Omega} (m_{\text{int}} - m_{\text{ext}}) \left( [B^T(m_0)B(m_0)]^{-1} B(m_0)r \right) ds(x) \quad (9)$$

When we substitute (9) into (1) we get our final update equation for our implicit surface

$$\frac{\partial \phi}{\partial \tau} = (m_{\text{int}} - m_{\text{ext}}) \left( [B^T(m_0)B(m_0)]^{-1} B(m_0)r \right) \Big| \vec{\nabla} \phi|. \quad (10)$$

## Second-order shape optimization

### General evolution algorithm

Our algorithm takes the following form:

```

Initialize  $\phi$ ,  $m_{ext}$ ,  $\Psi_{old}$ 
 $r \leftarrow$  calculate residual
for  $it = 1, niter$  do
   $\Psi_{new} \leftarrow \|r\|^2$ 
  if  $\Psi_{new} < \Psi_{old}$  then
     $g_{vel} \leftarrow B^T r$ 
     $g_\phi \leftarrow K(g_{vel})$ 
     $\beta_{max} \leftarrow$  find max step size
     $g_{DRLSE} \leftarrow$  calculate DRLSE
     $\phi_{it+1} = \phi_{it} + \beta_{max} \cdot g_\phi + g_{DRLSE}$ 
     $r \leftarrow$  calculate residual
  else
     $\beta \leftarrow$  line search
     $\phi_{it+1} = \phi_{it} + \beta \cdot g_\phi + g_{DRLSE}$ 
     $r \leftarrow$  calculate residual
  end if
end for

```

First we initialize our implicit surface, background velocity, and subsequently our full velocity model. Next, we compute synthetic data based on that full velocity model. After this operation we find our data residual and calculate our objective function value. We check to make sure the objective function value is decreasing for following iterations, but not the first. If so, then we compute a gradient using the adjoint Born operator. We use the conjugate gradient method to compute the application of the inverse of the Gauss-Newton Hessian on the FWI gradient calculated previously. Next we compute the search direction of the implicit surface (the K operator described in the algorithm above), as well as the maximum step size for our line search in a manner that satisfies the Courant-Friedrichs-Lewy (CFL) condition. By default, we take a step using the maximum stable  $\beta$  step size. If that step size lowers our objective function value, we proceed to calculate a new residual and gradient. But if it fails, then we undo our update and perform a line search to find an optimal  $\beta$  value instead of using the maximum  $\beta$ . We then use the optimal  $\beta$  to scale the implicit surface search direction. We also add a DRLSE (Distance Regularized Level Set Evolution) term in order to stabilize the evolution of the implicit surface. The functionality of this term is described at length in (Li et al., 2010). The  $\beta$  value is already calculated in a way that accounts for this DLRSE term. Last, the update is applied to the model, new synthetic data and residuals are made, and a new gradient is calculated for the next iteration.

### APPLICATION

We begin by using a perturbed starting model, and then use a fixed step-size steepest descent approach to get a reasonably close convergence to the true model. It is the result of this step that is the starting model used for the following examples. This initial attempt at convergence gives us a model where the more difficult features (like overhangs, or steep salt flanks) are still in need of correction (see Figure 2), and where the top of

salt regions are established, as is often the case an exploration imaging project.

We use a trailing line acquisition with 59 shots, each with 240 receivers. The receiver spacing is 25 [m], and the shot spacing is 100 [m], giving us 6100 [m] of offset. We use a shallow water bottom at 100 [m], making our model similar to a North Sea marine environment.

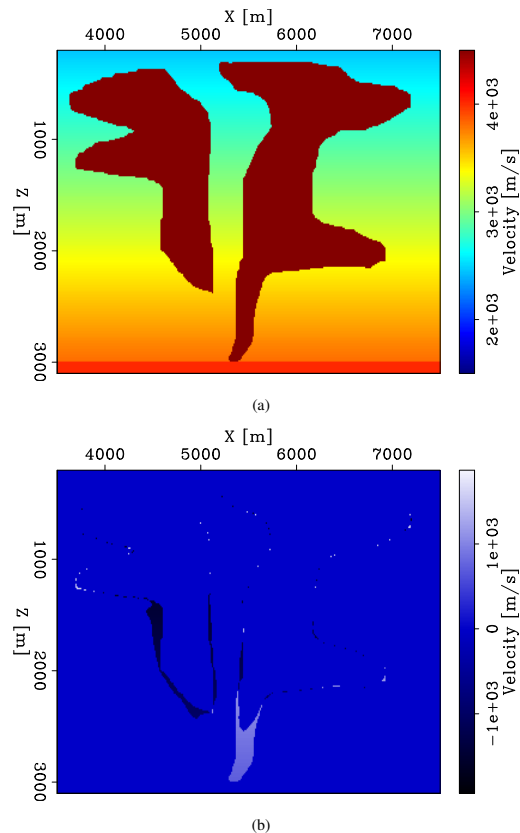


Figure 2: (a) True model (zoomed in); (b) Difference between full true model and initial guess.

We can see the specific areas where the two methods differ by looking at the differences between the updates that have been made to the model using either method. This is shown in 3. These changes are actually quite small, but show that the Hessian updating method does a better job at model convergence on some of the areas that are otherwise poorly illuminated, particularly at the base of the left salt body, as well as under the overhang.

When we look at the decrease in the objective function over iteration, we can see that the Gauss-Newton method correctly decreases faster than our steepest descent approach, for both the model residual norm (4) and the data residual norm (5). We used the same line search algorithm (quadratic interpolation) for both cases. However, in this comparison, the steepest descent norm curves make a notable jump at iteration 11. This jump occurs for a case where the algorithm reaches a local minima, such that the line search chooses a step size of zero. Since making this step size is pointless, we design the algorithm to

## Second-order shape optimization

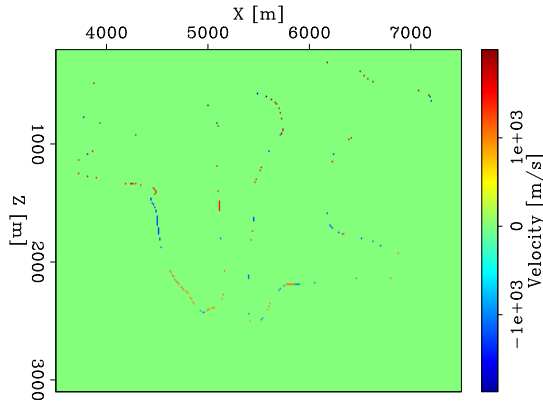


Figure 3: The difference between the absolute value of the changes made by each method, i.e.:  $(\text{ABS}(\text{Hessian\_result} - \text{true\_model}) - \text{ABS}(\text{Steepest\_descent\_result} - \text{true\_model}))$ . This plot can be interpreted as red areas being regions where the Gauss-Newton method performs best, and blue being where steepest descent performs best.

instead choose a small step size that will attempt to get us out of the local minima and continue descent. In this case the approach is mostly successful, and we continue to decrease the model norm accordingly. We choose to use the largest stable step size for each iteration, and then check to see if a reduction in the objective function is achieved. When it is not, we discard that update and redo it using a line search for the optimal step size. This is done for efficiency, as a line search for many of the iterations would otherwise choose the maximum step size anyway.

By utilizing a full implementation of the Hessian rather than a Gauss-Newton approximation, we would expect to be able to account for interaction between model parameters, which will further improve updating in areas where second-order scattering dominates, such as salt canyons, or other more complex geometries.

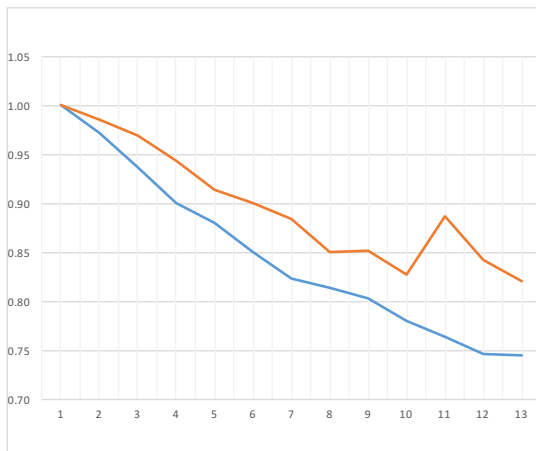


Figure 4: Comparison between the norm of the model residual for each method. Red is steepest descent method, while blue is the Gauss-Newton Hessian method.

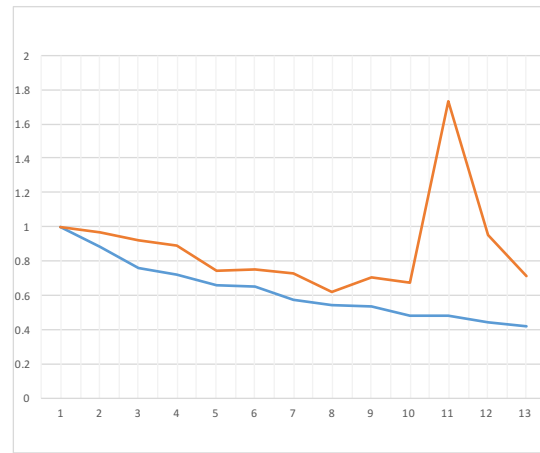


Figure 5: Comparison between the norm of the data residual for each method. Red is steepest descent method, while blue is the Gauss-Newton Hessian method.

### CONCLUSIONS

In conclusion, we find that by using second order information in our updating of the implicit surface, we gain improved convergence of our model, both in terms of the model residual norm and the data residual norm. However, one aspect that we must contend with is the increased cost of inverting the Hessian, and whether that cost is worth the improvement that we see.

### ACKNOWLEDGMENTS

Taylor would like to acknowledge the constructive conversations had with colleagues in the Stanford Exploration Project (SEP), especially Guillaume Barnier, Ettore Biondi, and Musa Maharromov. Further, we are grateful to SEP sponsors for both their technical advice and financial support.

## EDITED REFERENCES

Note: This reference list is a copyedited version of the reference list submitted by the author. Reference lists for the 2016 SEG Technical Program Expanded Abstracts have been copyedited so that references provided with the online metadata for each paper will achieve a high degree of linking to cited sources that appear on the Web.

## REFERENCES

- Burger, M., 2003, A framework for the construction of level set methods for shape optimization and reconstruction: *Interfaces and Free Boundaries*, **5**, 301–329, <http://dx.doi.org/10.4171/IFB/81>.
- Dahlke, T., B. Biondi, and R. Clapp, 2015, Domain decomposition of level set updates for salt segmentation: 85th Annual International Meeting, SEG, Expanded Abstracts, chapter 262, 1366–1371, <http://dx.doi.org/10.1190/segam2015-5917368.1>.
- Etgen, J., S. H. Gray, and Y. Zhang, 2009, An overview of depth imaging in exploration geophysics: *Geophysics*, **74**, no. 6, WCA5–WCA17, <http://dx.doi.org/10.1190/1.3223188>.
- Guo, Z., and M. de Hoop, 2013, Shape optimization and level set method in full waveform inversion with 3D body reconstruction: 83rd Annual International Meeting, SEG, Expanded Abstracts, 1079–1083, <http://dx.doi.org/10.1190/segam2013-1057.1>.
- Lewis, W., B. Starr, and D. Vigh, 2012, A level set approach to salt geometry inversion in full-waveform inversion: 82nd Annual International Meeting, SEG, Expanded Abstracts, <http://dx.doi.org/10.1190/segam2012-0737.1>.
- Li, C., C. Xu, C. Gui, and M. Fox, 2010, Distance regularized level set evolution and its application to image segmentation: *IEEE Transactions on Image Processing*, **19**, 3243–3254.
- Osher, S., and J. A. Sethian, 1988, Fronts propagating with curvature-dependent speed: Algorithms based on Hamilton-Jacobi formulations: *Journal of Computational Physics*, **79**, 12–49, [http://dx.doi.org/10.1016/0021-9991\(88\)90002-2](http://dx.doi.org/10.1016/0021-9991(88)90002-2).
- Plessix, R.-E., 2006, A review of the adjoint-state method for computing the gradient of a functional with geophysical applications: *Geophysical Journal International*, **167**, 495–503, <http://dx.doi.org/10.1111/j.1365-246X.2006.02978.x>.
- Santosa, F., 1996, A level-set approach for inverse problems involving obstacles: *ESAIM: Control, Optimisation and Calculus of Variations*, **1**, 17–33, <http://dx.doi.org/10.1051/cocv:1996101>.